Egypt. J. Chem. **Vol. 68**, No. 12 pp. 389 - 402 (2025)

Egyptian Journal of Chemistry

http://ejchem.journals.ekb.eg/

Mitigation of Fines Migration in Sandstone Reservoirs using Nanomaterials: An Experimental Case Study from Abu Rawash Formation-C Member, Western Desert, Egypt

Khalid M. Hamed[1], Abdulaziz M. Abdulaziz[2*], Ahmed Noah[3], and Osman Abdelghany[4]

[1]*Egyptian National Petroleum For Exploration and Development Company, Al Safwa Towers, Tower No.1 , 7th floor, Zaraa Nasr city, Cairo, Egypt*

[2]*Mining, Petroleum and Metallurgical Engineering Department, Faculty of Engineering, Cairo University, Giza, 12316, Egypt*

[3]*Egyptian Petroleum Research Institute, Ahmed El-Zomor Street - El Zohour Region, Nasr city, Cairo, 11727, Egypt*

[4]*Geology Department, Faculty of Science, Ain Shams University, Cairo, Egypt*

Abstract

Sand production is a major problem in petroleum industry. In this study, alumina (Al_2O_3) and silica (SiO_2) nano-fluids at different concentrations (0.1–0.6 g/L) and various flow rates (1–40 cm^3/min) were injected into two sandstone Cores to evaluate the effect of the nanomaterials on preventing fines migration. Core porosity and permeability were measured at each step to monitor changes and assess the effect of nano-fluids on Core properties. The optimal concentration of Al_2O_3 and SiO_2 nanomaterials for holding most of fines in place and producing a minimum quantity of fines was 0.4 g/L for both sandstone samples of Abu Rawash formation. The free fines in sandstone were entrapped by the electrostatic force of adsorption between the metallic oxides and the clayey fines. Monitoring the permeability of the Core plugs indicated a significant reduction in the permeability with increasing concentration of the injected nanomaterial, reflecting the entrapment of fines in the pores and plausible pore-neck plugging. New terms were proposed to characterize the produced fines weight into a specific number of a definite grain size: clay particle equivalent and the fine sand particle equivalent. Nanoparticles show promise in solving the issue of fines production and can be extended to other applications in the future of petroleum-oriented nanotechnology.

Keywords: Nanoparticle stability; Fines migration; Abu Rawash sandstone reservoir; Silica Nanoparticles; Alumina Nanoparticles.

1. Introduction

The evaluation, remediation, and control of sand production are challenging for efficient oil and gas production and reservoir management [1]. Fine migration can be attributed to numerous mechanisms, including chemical, physiochemical, hydrodynamic, biological, and thermal interactions of particles in formations with fluids, and the mechanical deformation of formations [2], [3]. Fines in sandstone formations consist of unconsolidated and loose particles within pore spaces, typically small enough to pass through pore throats [4], [5]. Particles, usually smaller than 37 μm, can migrate through fluid flow within sandstone reservoirs, causing pore plugging and reduced permeability [6]. Fines can be grouped as charged particles versus non-charged, clay versus non-clay, or naturally deposited versus artificially introduced while wellbore construction.

Lemon et al. showed that the change in the salinity of the pore fluid is the major chemical effect for the mobilization of fines in oil reservoirs [7]. The coexistence of clay and fresh water in geological units may initiate clay swelling, migration, and pore plugging, which ultimately contribute to significant fines migration [8], [9]. Khilar and Fogler [10] reported that the hydrodynamic force is the main factor driving fine migration at high flow rates while salinity generally plays a major role in fines movement, considering 4125 ppm as critical formation water salinity that can prevent permeability deterioration due to fines movement. Furthermore, pH can initiate fine detachment and liberation under lower pH conditions that prevail while acid treatment jobs. Alternatively, Gruesbeck and Collins [11] evaluated the permeability decline with the flow rate and concluded that formation damage due to fines migration can be mitigated when fluids flow below the critical flow rate. Locally, the detachment of fines is driven by many surface forces, including the double-layer effect, van der Waals attraction, Born repulsion,

*Corresponding author e-mail: amabdul@cu.edu.eg.; (Abdulaziz M. Abdulaziz).

Received date 11 February 2025; revised date 03 April 2025; accepted date 18 April 2025

DOI: 10.21608/ejchem.2025.359857.11299

and hydrodynamic forces. Typically, fines become detached when the repulsive force exceeds the attractive forces at the pore surface, with an overall positive total energy of interaction between the pore surface and the fines [12], [13].

Since the end of the 1980s, nanotechnology has been applied in the development of new nanomaterials by rearranging molecules and atoms [14]. Owing to the small size of nanoparticles (1–100 nm), their thermal, optical, chemical, and structural properties are completely different from those of either their atoms or bulk materials [15]. Nanoparticles are characterized by a large surface-area-to-volume ratio and small size and can be localized i small pore throats without affecting the porosity and permeability of formations [16]. As a result, researchers have proposed using nano-fluids to control fines migration. Huang et al. treated proppant particles using a nano- SiO_2 fluid to reduce the migration of fines by strengthening the attractive forces that fix suspended fines to porous media [17]. Similarly, Ogolo et al. [18] utilized aluminum oxide nanoparticles to attach clay fines to sand grains, thereby preventing the migration of fines. Other nanoparticles, including zinc oxide, nickel oxide, zirconium oxide, silane-treated silicon oxide, and magnesium oxide, enabled the successful control of fines migration. However, the coexistence of crude oil has a drastic negative impact on the performance of silane-treated silicon oxide and zinc oxide in controlling fines migration. Zinc oxide and magnesium oxide tend to reduce the permeability of formations by blocking the pore spaces [18].

Using different concentrations of nano- SiO_2 can reduce the migration of fines and increase the critical flow rate [19]. However, the effect of modifying the surface of sand grains is not well understood [20]. In an experimental study, three types of nano- SiO_2 were used: SiO_2 in deionized water (DIW), SiO_2 in DIW with a stabilizer (3-mercaptopropyl trimethoxy silane), and sulfonate-functionalized SiO_2 in DIW. SiO_2 nanoparticles not only reduced the migration of fines but also improved the water injectivity in Berea sandstone [20]. The effects of SiO_2, Al_2O_3, and MgO nanoparticles on fines migration [21], [22], [13] were investigated, demonstrating that MgO nanoparticles can control the movement of fines at different flow rates to a greater extent than other nanomaterials. Similarly, Assef et al. [23] reported the ability of MgO nanoparticles to control fine migration with minimal damage to formations. Furthermore, a SiO_2 nano-fluid with optimal concentration may improve the recovery factor for petroleum reservoirs. The ultimate recovery of the oil initially in place increased by approximately 13.28%, while tertiary flooding with 0.1 wt% SiO_2 nano-fluid was higher than that achieved by water flooding alone [24]. The SiO_2 nanoparticles can enhance oil production through various displacement or disjoining pressure mechanisms and wettability alterations. The disjoining pressure mechanism is usually dominant, in which SiO_2 nanoparticles in the dispersing medium are rearranged in a wedge-shaped film in contact with the discontinuous oil phase [25], [26]. This film separates the oil phase from the coalescence, contributing to the recovery of oil. The disjoining pressure is the pressure difference between the wedge-film pressure and bulk-liquid pressure [27]. The wettability alteration mechanism is dominant, where SiO_2 nanoparticles change the wettability of the rock, reduce the contact angle, and decrease the interfacial tension between two immiscible fluids [28], [29], [30]. To avoid the limitations of conventional acidification, Rafael et al. suggested a technique that uses agents to control fines migration, combined with the mitigation of fines migration using non-acid-based fluids [31], [32]. The effect of temperature on fines migration in sandstone during water disposal was evaluated at three different temperatures (25, 50, and 70° C), where the results showed a reduction in the fines migration with increasing temperature [33]. This behavior is explained by the increasing solubility of Ca^{++} ions in water as the temperature increases, associated with the dissolution of carbonate minerals at the pore throats, which consequently increases the permeability [33].

The present study aims to experimentally evaluate the effect of nano-fluids on fine migration on two sandstone Core samples using two types of nanoparticles: SiO_2 and Al_2O_3 nanoparticles. The concentration and flow rate of the nanoparticles in each Core are systematically varied to monitor the changes in fines migration in clastic reservoirs. Such an evaluation is crucial for optimizing the economics of well production and reservoir management [34].

2. Materials and Methods

Materials

Two Abu Rawash C-member sandstone Cores, which are potential subsurface reservoir units with different permeability ranges, were selected from the Western Desert in Egypt for the present study. The Core porosity (31.95 and 31.15%) and permeability (1381.08 and 448.42 milli Darcy, mD) were measured in samples #1 and #4, respectively, and results are listed in **Table 1** with other physical properties. The two Core samples are sandstone with lithofacies mainly quartz arenite to subarkose microfacies of fine- and medium-grained textures. The main clasts are made of monocrystalline and polycrystalline quartz (more than 85% of the total volume of the rock) and feldspar grains of plagioclase and microcline (5-10% of the total volume). Mica grains are mainly muscovite and occur in subordinate amounts. The matrix reaches up to 5% but does not exceed 7% and is mainly represented by fine-grained quartz and clay particles in the two core samples. The clasts are angular to subangular, sub-elongate, and moderately sorted. Occurrence of fine-grained materials is related to alteration of mica grains and disintegration of some quartz grains. The clasts show elongated grain packing due to a slight compaction. Few pore-filling iron oxides occur as intergranular cement between the clasts. The mineralogical composition was determined by X-ray diffraction (**Table 2**), confirming a relatively homogeneous composition with a slightly higher content of clay, carbonates, and pyrite in Core #4. Two types of nanoparticles were used: SiO_2 and Al_2O_3 nanoparticles with a particle size of 20–30 nm. The SiO_2 and Al_2O_3 nanoparticles were amorphous and spherical, respectively.

Table 1: Petrophysical Core data and measurements.

Sample No.	Pore Volume cm^3	Bulk Volume cm^3	Height cm	Diameter cm	Permeability mD	Grain Density g/cm^3	Porosity %
4	10.32	33.13	3	3.75	448.418	2.58	31.15
1	17.64	55.2	5	3.75	1381.082	2.6	31.95

Table 2: Semi-quantitative XRD results of Core samples (1 and #4)

Clay	Quartz	Alkali Feldspar	Calcite	Dolomite	Pyrite	Total
Core #1						
1.74%	90.98%	5.10%	1.24%	0.29%	0.65%	100%
Core #4						
2.59%	88.98%	5.55%	1.54%	0.49%	0.85%	100%

Methods

A brine solution (50 g/L NaCl) served as the dispersion medium for the nanoparticles and was deployed as the production fluid before and after injecting the nanomaterial. The nanoparticles were dispersed in the brine at concentrations of 0.1, 0.15, 0.2, 0.3, 0.4, and 0.6 g/L. The two types of nano-fluids, Al_2O_3 and Al_2O_3, were used in varying concentrations, with SiO_2 injected first, followed by aluminium oxide. The laboratory procedures are illustrated in **Fig. 1**. The Core was cleaned and dried before measuring porosity and air permeability, then saturated with 50 g/L brine. The production simulation started at different flow rates (5, 10, 15, 20, 25, 30, 35, and 40 cm^3/min), which ensured that ~15 pore volume (PV) was produced at each flow rate. The produced fluid was collected and filtered using filter paper to separate the produced fines. Finally, the sand produced was dried and weighed for each run. Thereafter, the injection of Al_2O_3 nano-fluid was started at a concentration of 0.1 g/L, with a total volume equivalent to the PV of the Core. The samples were then soaked under static conditions for approximately 6 hours. The production simulation for the 0.1 g/L Al_2O_3 nano-fluid was continued at a rate of 5 cm^3/min to ensure a total production of 15 PV. The produced fines were weighed as described for the blank (50 g/L brine), and the production simulation was repeated for the other assigned flow rates (10, 15, 20, 25, 30, 35, and 40 cm^3/min). The entire laboratory experiment was repeated for both Core samples using different concentrations and flow rates of SiO_2 nano-fluid. All experimental work was completed in the laboratories of Datalog, Egypt. **Fig. 2** presents a schematic of the experimental setup.

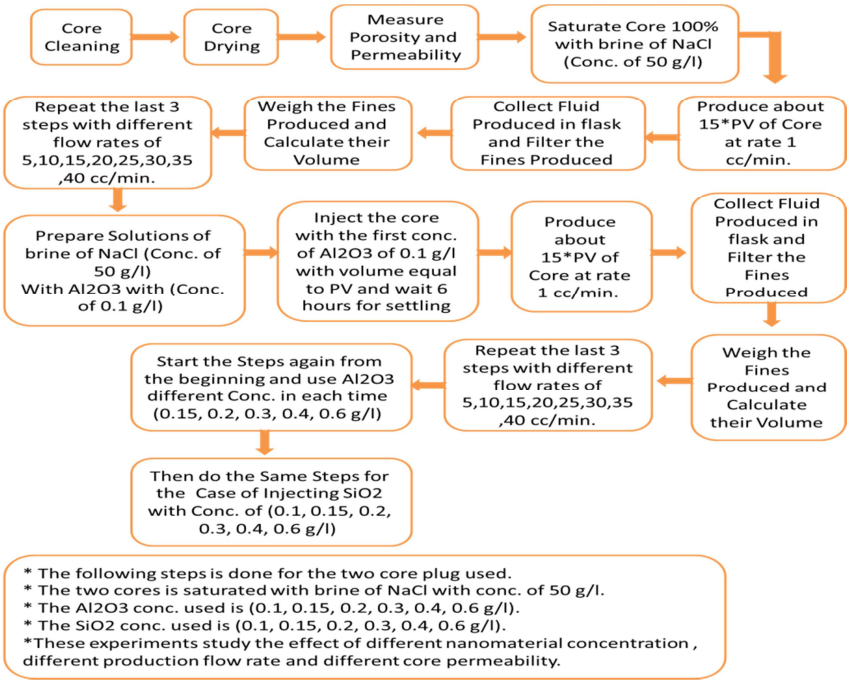

Figure 1: A Flow chart for experimental lab procedures.

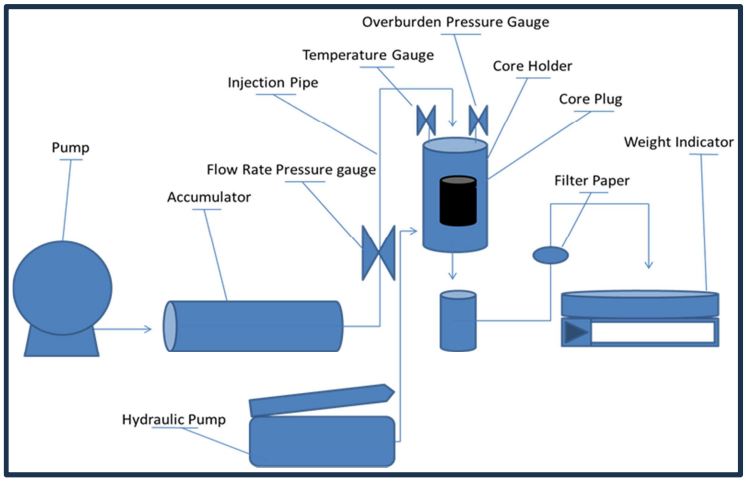

Figure 2: A schematic illustration of the experimental setup**.**

To identify the optimum nano-fluid concentration at a specific flow rate for achieving the highest reduction percentage of the produced fines, the weights of the sand produced at each flow rate before and after nano-fluid injection are compared. In addition, particle size (clay- and fine sand-) equivalent is proposed in the present study to present produced weight of fines in the form of number of the produced clay particle equivalent and/or fine sand particle fines. Given the total weight of the produced fines of any experiment, the number of produced particle equivalents can be calculated using the size of clay or fine-grained sand particles. This assumption is reasonable given the difficulty in specifying the exact size of the movable particles (the amount of clay versus fine sand). Using the average clay and fine sand grain density and diameter, known for the two Cores, together with the total produced fines weight, the number of clay particle equivalents or fine sand particle equivalents can be calculated and subsequently used to evaluate the produced fines. The following mathematical calculation sequence was used to determine the clay and fine sand equivalents:
Clay particle diameter = 0.0004 cm
Clay particle volume = 2.68×10^{-10} cm^3
Clay density = 1.702 g/cm^3
Weight of a single clay particle = 4.56×10^{-10} g
Diameter of a fine sand grain = 0.0062 cm
Volume of a fine sand grain particle = 10^{-6} cm^3
Fine sand grain density = 2.6 g/cm^3
Weight of a fine sand particle = 2.6×10^{-6} g

$$Sand\ or\ Clay\ particle\ equivalent\ =\ Total\ fines\ weight/single\ sand\ or\ clay\ particle\ weight$$

During the experiment, each Core was placed in a core holder under atmospheric pressure and injection/production was achieved using pumps. The produced fluids were collected in a graduated flask, filtered, and weighed. Atmospheric pressure conditions are preferred for this laboratory work to reduce the effect of high pressure on holding formation fines, thereby facilitating fines migration. Thus, the entrapment of fines by nano-fluids is expected to be more efficient in high-pressure environments [18]. All laboratory tests on the Al_2O_3 and SiO_2 nano-fluids were performed on the same Core plug to avoid the effects of numerous factors that control the movement of fine particles in the presence of nanomaterials. These factors include variations in the plug petrofabrics, wellbore drainage effects, the nature of the injected nanomaterial (multistage), and pore plugging effects. Variations in plug petrofabrics occur in plugs of the same Core because of variations in the pore patterns and deformation features at the grain scale. The most common features include petrofabric constituents and textures, fractures (distribution, morphology, and orientation), crystal twinning, pressure solutions, and recrystallized fabrics. Such variations in the pore patterns and deformation mechanisms effectively affect the migration of fines, porosity, and permeability [35]. The wellbore drainage effect prevails when nanomaterials are injected into the formation because the area around the wellbore typically receives more nanoparticles than that located away; consequently, the concentration of the injected nanomaterial would be higher near the wellbore compared to that at the area around the well boundary. Therefore, nano-fluids at various concentrations were injected into the same Core plug to simulate the dominant situations around injection borehole where the concentration varies in the vicinity of the wellbore. Thus, during the test it is possible that some of the injected nanoparticles remain in the plug lead to concentration variations around the wellbore when the next (subsequent) concentration of nanofluid is injected. The multistage concentration of the injected nanomaterial appears justified, especially when various nanomaterial concentrations are used during multistage nano-fluid treatment. The pore-plugging effect typically accounts for erroneous results when the Core is treated only once, as the produced fines may plug the pores at the boundary of the plug, possibly resulting in low permeability and associated low sand production. This problem was avoided by working on the same plug many times at different flow rates and concentrations. In consequence,

the possibly plugged pores would have been unplugged by the turbidity effect, turbulent flow, flow diversion, or other flow mechanisms. Moreover, the results of tests on two Cores with different properties were found to be inconsistent due to changes in pore pattern, physiochemical conditions, and prevailing flow mechanism. Alternatively, the use of several Cores enables analysis of the permeability effect on the activity of the nanomaterial. However, in such cases, other factors, including geological heterogeneity and inconsistencies in the flow media effect, are normally ignored.

3. Results and Discussion

Effect of nano-fluid concentration on fines production

Numerous factors contribute to the mobility or retention of fines, which may be related to the physical characteristics of the particles (e.g., surface area, size, and electrical charge) and/or ambient environmental conditions, including the characteristics of the saturating fluid, temperature, organic matter content, dissolved metals, and inorganic colloids [36], [37]. In the present study, the effect of injecting nanomaterials at different concentrations on the production of fines was evaluated for two Core samples by weighing the produced fines before and after injection of the nanomaterial. A comparison of the results for all Al_2O_3 and SiO_2 concentrations showed that the maximum reduction in the fines production was observed at a concentration of 0.4 g/L. For comparison, the results with 0.1 and 0.4 g/L of both Al_2O_3 and SiO_2 nano-fluids are presented. **Tables 3–4** and **5–6** present the fines production in both Core samples with 0.1–0.4 g/L concentrations of Al_2O_3 and SiO_2, respectively. Injection of 0.1 g/L Al_2O_3 nano-fluid in Core #4 reduced fines production by 41.7–55%, with a maximum reduction of 55% at 1 cm³/min. In Core #1, the production of the fines was reduced by 30.3–35% and changed minimally with a variation of the flow rate within the studied range. **Table 4** shows a percentage fines reduction of 97% in Core #4, which remained acceptable (89.6%) at a flow rate of 15 cm^3/min. A similar trend was reported for Core #1, with a 96.9% reduction in the fines production at a flow rate of 1 cm^3/min, which remained relatively high (91.5%) at a flow rate of 15 cm^3/min.

Table 3: Core #1 and Core #4 fines production over different production rates before and after injection of 0.1 g/L Al_2O_3 nano-fluid.

Al_2O_3 of 0.1 g/L						
Production Flow Rate	**CORE 4**			**CORE 1**		
	Before Injection (mg)	**After Injection (mg)**	**Prod. Fines Reduction (%)**	**Before Injection (mg)**	**After Injection (mg)**	**Prod. Fines Reduction (%)**
1cm^3/min	0.378	0.170	55 %	0.314	0.210	33.1 %
5cm^3/min	0.390	0.177	54.6 %	0.354	0.224	36.7 %
10cm^3/min	0.412	0.185	55.1 %	0.375	0.245	34.7 %
15cm^3/min	0.422	0.201	52.4 %	0.392	0.260	33.7 %
20cm^3/min	0.428	0.204	52.3 %	0.423	0.295	30.3 %
25cm^3/min	0.440	0.211	52.0 %	0.441	0.285	35.4 %
30cm^3/min	0.465	0.241	48.2 %	0.466	0.310	33.5 %
35cm^3/min	0.477	0.265	44.4 %	0.485	0.312	35.7 %
40cm^3/min	0.496	0.289	41.7 %	0.512	0.333	35 %

Table 4: Core #1 and Core #4 fines production over different production rates before and after injection of 0.4 g/L Al_2O_3 nano-fluids.

Al_2O_3 of 0.4 g/L						
Production Flow Rate	**CORE 4**			**CORE 1**		
	Before Injection (mg)	**After Injection (mg)**	**Prod. Fines Reduction (%)**	**Before Injection (mg)**	**After Injection (mg)**	**Prod. Fines Reduction (%)**
1cm^3/min	0.088	0.002	97.7 %	0.128	0.004	96.9 %
5cm^3/min	0.092	0.006	93.5 %	0.132	0.006	95.5 %
10cm^3/min	0.094	0.09	90.4 %	0.138	0.014	89.9 %
15cm^3/min	0.096	0.010	89.6 %	0.141	0.012	91.5 %

20cm^3/min	0.103	0.015	85.4 %	0.143	0.019	86.7 %
25cm^3/min	0.106	0.022	79.2 %	0.146	0.021	85.6 %
30cm^3/min	0.101	0.028	72.3 %	0.151	0.023	84.8 %
35cm^3/min	0.110	0.033	70.0 %	0.159	0.034	78.6 %
40cm^3/min	0.121	0.039	67.8 %	0.161	0.038	76.4 %

Table 5: Core #1 and Core #4 Fines production over different production rates before and after injection of 0.1 g/L SiO_2 nano-fluids

SiO_2 of 0.1 g/L						
Production Flow Rate	**CORE 4**			**CORE 1**		
	Before Injection (mg)	**After Injection (mg)**	**Prod. Fines Reduction (%)**	**Before Injection (mg)**	**After Injection (mg)**	**Prod. Fines Reduction (%)**
1cm^3/min	0.204	0.110	46.1 %	0.118	0.060	49.2 %
5cm^3/min	0.224	0.115	48.7 %	0.122	0.067	45.1 %
10cm^3/min	0.231	0.123	46.8 %	0.129	0.075	41.9 %
15cm^3/min	0.239	0.124	48.1 %	0.132	0.087	34.1 %
20cm^3/min	0.244	0.129	47.1 %	0.138	0.092	33.3 %
25cm^3/min	0.249	0.135	45.8 %	0.141	0.092	34.8 %
30cm^3/min	0.258	0.141	45.3 %	0.152	0.098	35.5 %
35cm^3/min	0.266	0.149	44 %	0.159	0.102	35.8 %
40cm^3/min	0.275	0.155	43.6 %	0.168	0.107	36.3 %

Table 6: Core #1 and Core #4 fines production over different production rates before and after injection of 0.4 g/L SiO_2 nano-fluids.

SiO_2 of 0.4 g/L						
Production Flow Rate	**CORE 4**			**CORE 1**		
	Before Injection (mg)	**After Injection (mg)**	**Prod. Fines Reduction (%)**	**Before Injection (mg)**	**After Injection (mg)**	**Prod. Fines Reduction (%)**
1cm^3/min	0.048	0.004	91.7 %	0.064	0.006	90.1 %
5cm^3/min	0.049	0.005	89.8 %	0.076	0.008	89.4 %
10cm^3/min	0.068	0.008	88.2 %	0.089	0.009	89.9 %
15cm^3/min	0.076	0.008	89.5 %	0.096	0.010	89.6 %
20cm^3/min	0.078	0.019	75.6 %	0.098	0.027	72.4 %
25cm^3/min	0.079	0.018	72.2 %	0.099	0.029	70.7 %
30cm^3/min	0.088	0.023	73.9 %	0.102	0.037	63.7 %
35cm^3/min	0.089	0.026	70.8 %	0.112	0.039	65.2 %
40cm^3/min	0.092	0.029	68.5 %	0.125	0.045	64 %

On injecting SiO_2 nanoparticles at a concentration of 0.1 g/L at the specified flow rates, the fines production was reduced between 43.6% and 48.7% in Core #4 (**Table 5**). The maximum percentage of reduction (46%) was achieved at a flow rate of 1 cm^3/min and remained constant up to a flow rate of 40 cm^3/min. In Core #1, the percentage fines reduction was between 33.3 and

49.2%, with the maximum value of 49.2% achieved at a flow rate of 1 cm^3/min, which decreased to 35% at a flow rate of 15 cm^3/min. For the Al_2O_3 nanoparticles, a nano-fluid concentration of 0.4 g/L (**Table 6**) enabled the optimal fine reduction throughout the experiment. In Core #4, the percentage fines reduction ranged from 68.5 to 91.7% over the entire range of studied flow rates, with 91.7% fines reduction at a flow rate of 1 cm^3/min. The reduction remained relatively high (89.5%) at a flow rate of 15 cm^3/min. However, in Core #1, fines production was reduced by 63.7–90.1% at a flow rate of 1 cm^3/min and remained relatively constant (89.6%) at a flow rate of 15 cm^3/min. The results primarily reflect the effect of the utilized nanoparticles on mitigating fine migration at a concentration of 0.4 g/L and the optimum flow rate of 15 cm^3/min. Such results depend on the capacity for adsorption of the nanomaterial on the surface of mobile fines under the dominant physicochemical conditions [37]. The adsorption capacity of materials normally varies with the type and characteristics of the adsorbed material; however, the adsorption mechanisms and influential chemical parameters are not well understood [38], [39]. Though, Arenas et al. [39] used the Langmuir isotherm to describe the adsorption process and described the kinetics with a pseudo-2nd order model. Further investigations of the physicochemical conditions prevailing flow in porous media systems are required to understand the thermodynamic aspects of adsorption that lead to the retention or mobilization of fines.

In the present study, new terms are proposed to numerically characterize the produced fines relative to the most common fine particles, clay and fine sand. The number of produced 'clay particle equivalent' and 'fine sand particle equivalent' are used to represent the weights of the produced fines in this experiment. Using the sequence of calculations presented in methodology, the number of clay particle equivalents and fine sand particle equivalents was calculated using the weight of the produced fines for an Al_2O_3 concentration of 0.4 g/L; the results are presented in **Table 7**.

Table 7: Number of equivalent clay and sand particles produced over different production rates after injection of 0.4 g/L Al_2O_3 nano-fluids in Core#1 and Core#4.

Al_2O_3 of 0.4 g/L				
Production Flow Rate	**Core 4**		**Core 1**	
	Clay Particles Produced*10^3 After Inj.	**Sand Particles Produced After Inj.**	**Clay Particles Produced*10^3 After Inj.**	**Sand Particles Produced After Inj.**
1cm^3/min	4.39	0.77	8.77	1.54
5cm^3/min	13.16	2.31	13.16	2.31
10cm^3/min	197.37	34.62	30.70	5.38
15cm^3/min	21.93	3.85	26.32	4.62
20cm^3/min	32.90	5.77	41.67	7.31
25cm^3/min	48.25	8.46	46.05	8.08
30cm^3/min	61.40	10.77	50.44	8.85
35cm^3/min	72.37	12.69	74.56	13.08
40cm^3/min	85.53	15.00	241.23	14.62

After injecting the nano-fluid, the mechanism by which the nanomaterial trapped the free fines that moved freely at different production flow rates was evaluated. This mechanism is plausibly related to the effect of polarization of nanomaterials, induced by the electrical charge on the metallic oxides (Al_2O_3 or SiO_2) in the injected solution. Zeta potential refers to the potential difference between the fluid layer surrounding a charged particle and the bulk fluid [40]. The magnitude of the zeta potential indicates the feasibility of coagulation of the suspended particles and the overall stability of the system. Suspension systems with large positive or negative zeta potentials comprise particles that repel each other and do not aggregate. Nevertheless, a suspension with a low zeta potential lacks such repulsive forces, and consequently, the suspended fines flocculate. Quartz sand particles in ultrapure water are negatively charged with a zeta potential that decreases progressively from 0 mV at a pH of 0.9−1.1 to –48.0 and −38.4 mV at pH 11.9−12.1; the zero-charge point is consistent with the values reported in the literature [41]. The zeta potential in real environmental conditions is always lower than that measured in ultrapure water at pH 8.0 (−35.0 mV). Therefore, fine sand (< 0.45 μm) with a negative charge can be easily stabilized by positively charged components [37]. The electrostatic force between the positively charged oxide particles and the negatively charged (−) clayey fines shown in **Fig. 3** may explain the entrapment mechanism [2]. In this case, the positively charged oxides act as electrostatic bridges between the existing negatively charged fines, ultimately resulting in the formation of large heterogeneous aggregates [37], [42]. In addition, the surface potential of suspended fine grains is typically less than that of rock grains; therefore, nanoparticles are attracted to the fine grains and are consequently adsorbed on their surface. This adsorption can alter the surface potential of the fine particles, resulting in a decrease in the repulsive force between the fines and rock grains. Thus, the injection of nanoparticles increases the adsorption of fine particles on the rock grains [13], [21], [43], [44]. However, the presence of dissolved organic matter can disturb the entire system either by increasing or decreasing the energy barriers based on the physiochemical conditions that influence the van der Waals attraction, controlling the aggregation/destabilization process [45], [46].

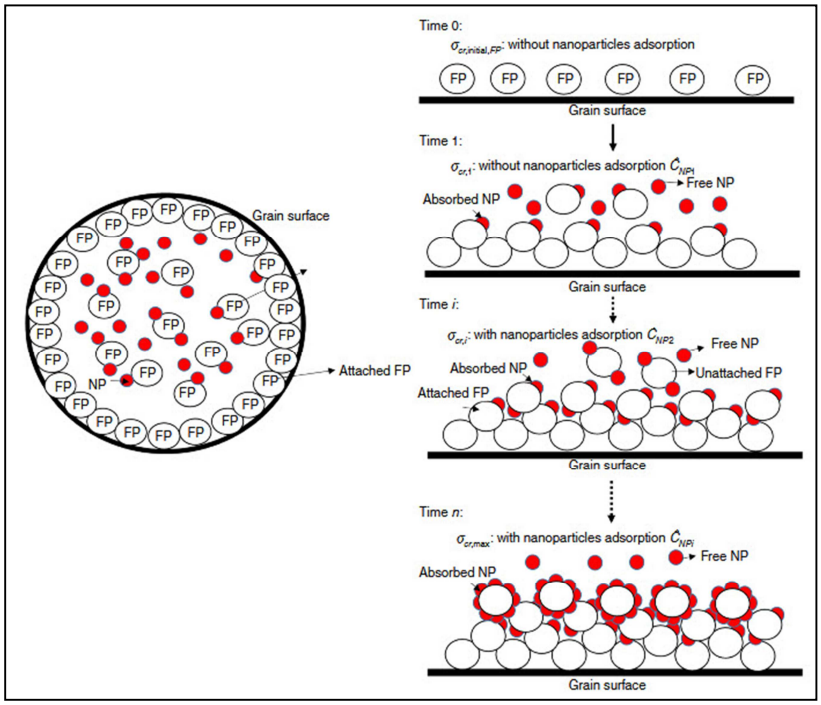

Figure 3: Adsorption mechanism of nanoparticles on the surface of suspended fines [2].

Effect of flow rate on fines production

After injecting the nano-fluids into the Cores, production was simulated at flow rates of 1–40 cm^3/min and the measured permeability of the Core versus the brine throughput of the Core is shown in **Fig. (4–7)** for the two Core samples when the Al_2O_3 and SiO_2 nano-fluids were injected. When Core #1 was flooded with the Al_2O_3 nano-fluid (**Fig. 4**) at concentrations of 0.1, 0.15, and 0.2 g/L, the maximum permeability (determined from the curve) was observed at a brine throughput of 2.15 L, with an average nano-fluid injection rate of 25 cm^3/min. However, at concentrations of 0.3, 0.4, and 0.6 g/L the curve showed high permeability at a brine throughput of 0.9 L, with an average fluid injection rate of 15 cm^3/min. After injection of Al_2O_3 into Core #4, the maximum permeability was observed at a brine throughput of 2.65 L at an average flow rate of 35 cm^3/min for concentrations of 0.1, 0.15, and 0.2 g/L (**Fig. 5**). Alternatively, at concentrations of 0.3, 0.4, and 0.6 g/L the curve showed a maximum permeability at a brine throughput of 1.7 L, with an average flow rate of 20 cm^3/min. The optimum flow rate for production at high permeability was obtained when the brine throughput is maximized. The peak flow rate was achieved at low concentrations rather than at high nanomaterial concentrations.

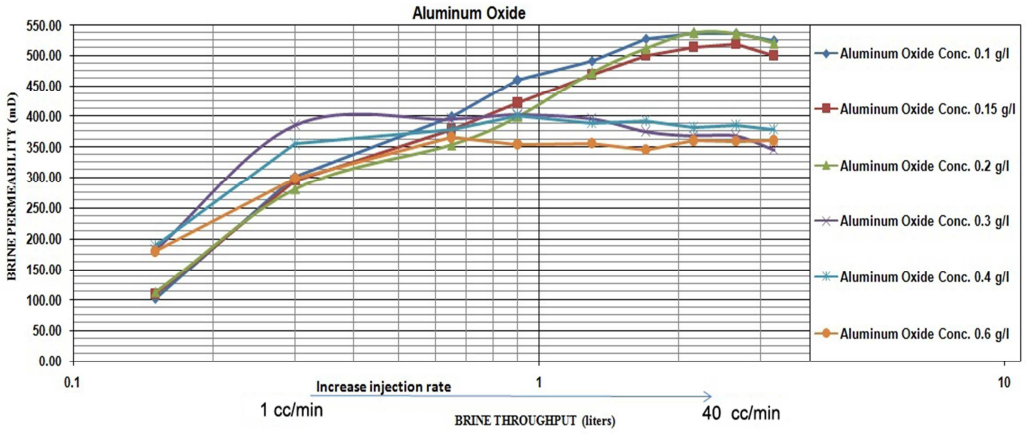

Figure 4: Brine throughput versus the brine permeability plot for injection of Al_2O_3 nano-fluids in Core #1.

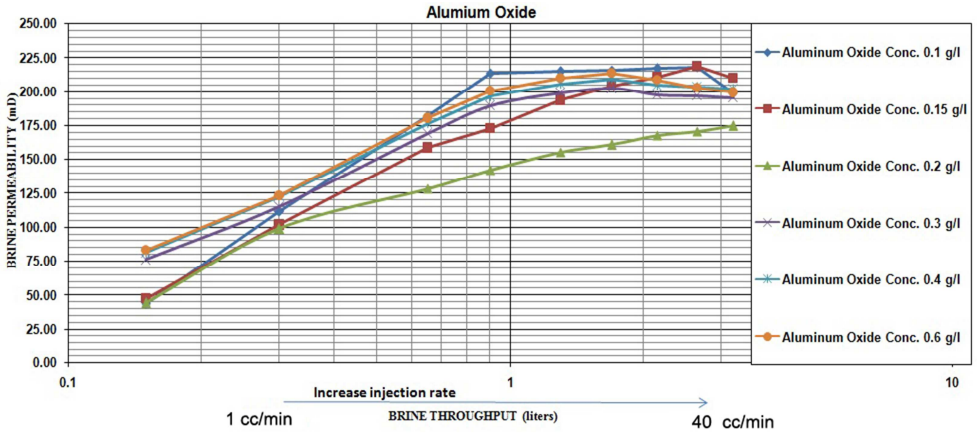

Figure 5: Brine throughput versus the brine permeability for injection of Al_2O_3 nano-fluids in Core #4.

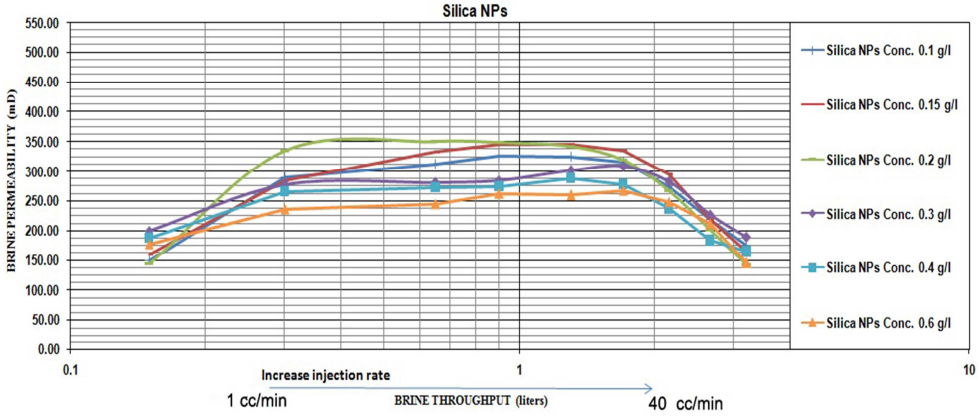

Figure 6: Brine throughput versus the brine permeability for SiO_2 nano-fluids injection in Core #1.

On injecting SiO_2 nano-fluids at concentrations of 0.1, 0.15, and 0.2 g/L into Core #1, the curve (**Fig. 6**) showed a maximum permeability at a brine throughput of 2.15 L, with an average flow rate of 25 cm^3/min. At concentrations of 0.3, 0.4, and 0.6 g/L, the permeability was maximal at a brine throughput of 0.9 L, with an average flow rate of 15 cm^3/min. Alternatively, with the injection of SiO_2 nano-fluids into Core #4, the fluid permeability increased as the injection rate of the nano-fluid increased (**Fig. 7**). At nano-fluid concentrations of 0.1, 0.15, and 0.2 g/L, the curve showed a maximum permeability at a brine throughput of 2.65 L, at an average flow rate of 35 cm^3/min. However, at concentrations of 0.3, 0.4, and 0.6 g/L, the curve showed a peak permeability at an average flow rate of 20 cm^3/min for a brine throughput of 1.7 L.

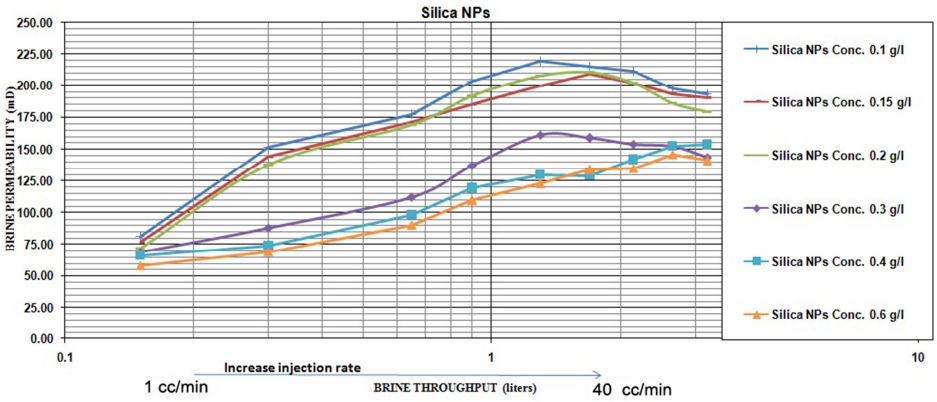

Figure 7: Brine throughput versus the brine permeability for SiO_2 nano-fluids injection in Core #4.

Typically, the adsorption capacity of quartz sand grains is lower than that of metal oxide nanoparticles [47], which explains the increasing trend in fines entrapment as the nano-fluid concentration increases. The adsorption capacity of both nanoparticles and sand grains is controlled by the contact time and dispersion, which are directly related to the flow rate. The contact time required to reach the optimum capacity for fine adsorption decreased as the moving fines increased at a constant nano-fluid concentration [37], [47]. Generally, the affinity of the surfaces of positively charged nano-oxides for a reservoir is attributed to electrostatic interactions. The capacity for the adsorption of fines increased as the nano-fluid concentration is increased. This behavior is explained by the prevailing greater mass driving forces capable of overcoming the transfer resistance. These forces facilitate fines coagulation and diffusion of the nanomaterial from the solution to the surfaces of the sandstone matrix [48]. As the mobility of the fines increases, the adsorption capacity decreases because of faster saturation of the active sites for adsorption on the nanoparticles, that is, blockage of the adsorption sites. This process is driven by the repulsive forces between individual fine particles on the nanoparticle/sandstone matrix, along with the increasing diffusion at higher nano-fluid concentrations and/or high flow rates [49]. Generally, the overall observed trend indicated that the permeability curve for any concentration increased to a peak, followed by a decline. This behavior can be explained by the movement and coalescence of fines with the nanoparticles, which increases the flow rate until the coalescence of fines approaches a pore neck, where blockage of the pore neck diverts the flowing fluids and decreases the permeability [50].

Effect of nano-fluid performance on effective permeability

After injecting the Al_2O_3 nano-fluids at different concentrations, the air permeability of each sample was measured and is subsequently compared with the original measured permeability at the beginning of the experiment. **Fig. 8** indicates a progressive increase in permeability during the testing of Core #4 with nano-fluid concentrations up to 0.3 g/L, after which permeability decreased over a wide concentration range due to the entrapment of more fines on the nanoparticles at the pore throats. However, in the case of Core #1, the permeability decreased at all concentrations of injected nanoparticles (**Fig. 9**). When the concentration of the injected nano-fluid exceeded 0.2 g/L, the permeability decreased sharply, preventing additional migration of the fines. Small pore spaces may be the main contributors to the permeability of sample #1, and therefore significant changes were observed upon injecting the nano-fluids, even at low concentrations. In contrast to sample #1, medium-to-large pore throats are the main contributors to the permeability of sample #4. These pore throats could manage the flow due to the increase in permeability with the injection of the nano-fluids up to a concentration of 0.3 g/L. The adsorption of mobile fine particles on the active sites of the nanoparticle surface is controlled by electrostatic interactions between the highly negatively charged fines and positively charged nanoparticles. Mobile fines adsorbed on the surface of the nanoparticles undergo lateral interactions induced by electrostatic repulsive forces. These forces facilitate the homogeneous distribution of the moving nanoparticle-fined clusters. Alternatively, the nanoparticles can act as electrostatic bridges between the mobile fines and rock matrices [51], [52].

On injecting SiO_2 nano-fluids of different concentrations into Core #4, the permeability increased up to a nano-fluid concentration of 0.3 g/L, followed by a permeability reduction over a wide concentration range (**Fig. 10**), which prevented additional fines migration. For Core #1, the permeability decreased at nano-fluid concentrations less than 0.3 g/L, compared to the original permeability, followed by a marked improvement in the permeability (**Fig. 11**). This behavior is explained by plugging tight pore throats that direct the flowing water stream to new channels and consequently improved permeability, in what is known as flow diversion. Over very small pore throats, the density difference between the nanoparticles and water molecules and the constant differential pressure in the pores resulted in slower movement of the nanoparticles compared to that of the water molecules. This led to the accumulation of the nanocomponents in the pore space, which finally plugs the nearest pore throats. Such pore-throat blockage increases the water phase pressure and eventually forces the flowing water to take other paths/routs through the pore systems that could, in some cases, cross non-moving (stagnant) oil phases. Such pressure build-up in adjacent pores of petroleum reservoirs forces stagnant oil to phase out, which ultimately improves the oil sweep efficiency in water flooding programs [53]. Once the oil is freed, the surrounding pressure drops, the blockage gradually dissociates, and consequently water flow through the inter-particle pore system commences [28], [29], [30], [54]. Compared to the published results in [55] (SiO_2 nanoparticles at concentration 0.5 g/l and flow rate of 3.0 cc/min) for Abu Rawash reservoir, the present study showed that the maximum permeability is achieved at comparatively less SiO_2 nano-fluid concentration (~0.3 g/L) but significantly higher flow rates of 15-35 cm3/min. Such a wide range of changes in flow rate and nano-fluid concentration is attributed to the effect of pore pattern change and probable changes in mineralogical composition.

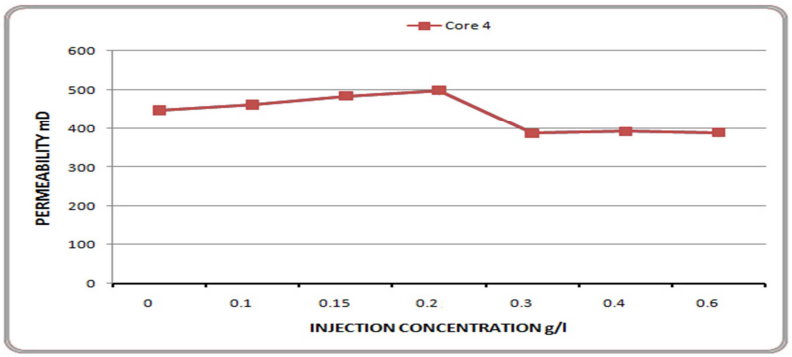

Figure 8: Brine permeability versus injection concentration for Al_2O_3 nano-fluids injection in Core #4.

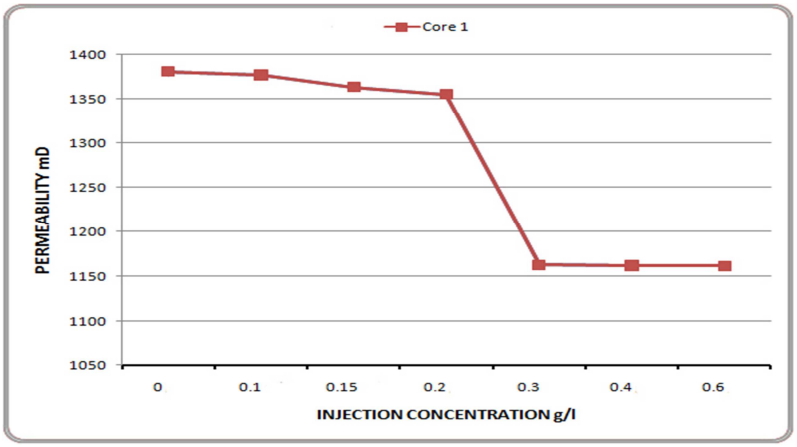

Figure 9: Brine permeability versus injection concentration for Al_2O_3 nano-fluids injection in Core #1.

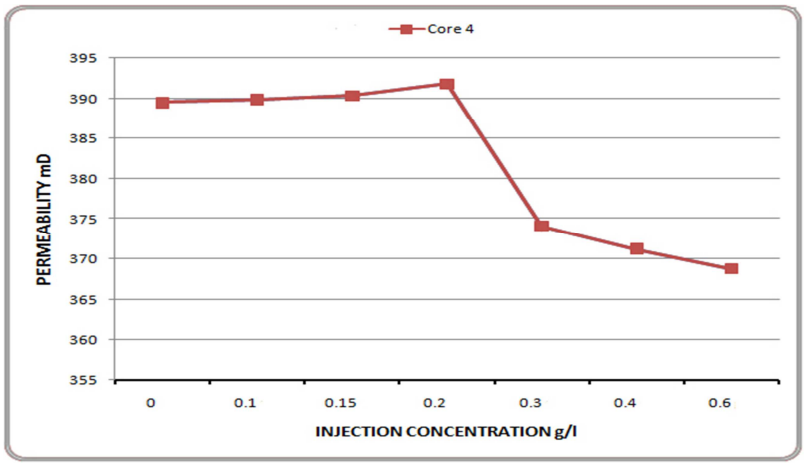

Figure 10: Brine permeability versus injection concentration for SiO_2 nano-fluids injection in Core #4.

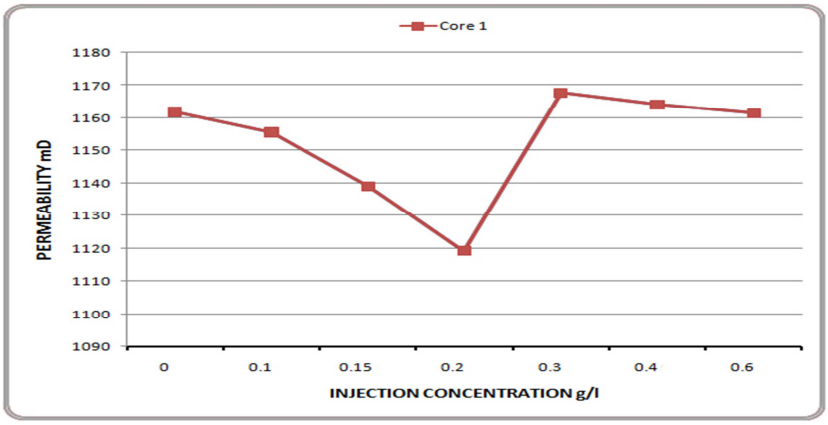

Figure 11: Brine permeability versus injection concentration for SiO_2 nano-fluids injection in Core #1.

4. Conclusion

Using two Core plugs with different permeabilities, the effectiveness of Al_2O_3 and SiO_2 nano-fluids at different flow rates and concentrations for mitigating the migration of fine particles was evaluated. The optimum concentration of the nano-fluids injected into the Core samples was 0.4 g/L for both Al_2O_3 and SiO_2, enabling a significant reduction in the produced fines and

entrapment of most of these fines. The present experiment considered a wide range of flow rates, from 1 to 40 cm^3/min. The results indicated a direct proportionality between fines migration and the flow rate. The optimum production flow rate with minimal production of fines using the optimum nano-fluids was 15 cm^3/min. Generally, the permeability of the Core plugs was inversely proportional to nanomaterial concentration, reflecting finer entrapment in the pores and possible pore-neck plugging. Core production was determined after injecting the nanomaterial, indicating an increase in the calculated brine permeability as the flow rate increased, with an ensuing decrease upon reaching the optimum flow rate. The clay particle equivalent and fine sand particle equivalent are new terms introduced in this study to characterize the weight of produced fines as particle numbers. The adsorption of nanoparticles on the surfaces of the fines and grains increased the retention of the fines because of the decreasing surface potential between the grains and fines and prevented the migration of more fines. Overall, the nano-fluids may improve fine production in sandstone reservoirs.

Acknowledgments
The authors acknowledge the support of the Faculty of Engineering, Cairo University during the progress of this work. Special gratitude to the Datalog laboratories in Egypt for providing the facility to complete experimental work and measurements. Cautious revision by Prof. Dr. Abdelzaher Abuzaid, Faculty of Engineering, Cairo University, is highly appreciated.

References

[1] Manhalawi A., Dahab A.S., Abdulaziz A.M., Abbas A.K., AL-Husseini N., 2020. *Wellbore stability evaluation for depleted reservoir*. 54th U.S. Rock Mechanics/Geomechanics Symposium. Virtual, Online28 June 2020 through 1 July 2020, Code 164331.
[2] Yuan B., Moghanloo R.G., and Zheng D., *Analytical Evaluation of Nanoparticle Application To Mitigate Fines Migration in Porous Media*, SPE J. 2016, 21, 2317–2332. doi: https://doi.org/10.2118/174192-PA.
[3] Abdelhak A.I., Ghanem A.F. Abdulaziz A.M., Kabel K.I., Noah A.Z., Youssef A.M., Dahab A., *Synthesis and Evaluation of Poly (isobutylene-alt-maleic anhydride)-co-Poly (ethylene glycol) and its Copper Oxide Nanocomposite for Enhancing the Performance of Water-based Drilling Fluids in HPHT Wells*. Egyptian Journal of Chemistry, 2022, 65(9), 349 – 360. 10.21608/EJCHEM.2022.111764.5075
[4] Muecke T.W., formation fines and factors controlling their movement in porous media. J. Petrol. Technol., 1979, 3, (2), 144–150. https://api.semanticscholar.org/CorpusID:108702762
[5] Gamal H.; Elkatatny S.; Abdulaziz A.M., Intelligent Solution for Auto-Detecting Lithology Scheme While Drilling by Machine Learning, International Petroleum Technology Conference, IPTC 2024, 10.2523/IPTC-24535-MS
[6] Civan F., Reservoir Formation Damage. Fundamentals, Modeling, Assessment, and Mitigation, second ed., Burlington, Massachusetts, Gulf Professional Publishing, 2007, pp. 1112.
[7] Lemon E.P., Zeinijahromi A., Bedrickovetsky G.P., et al., Effects of injected-water salinity on water flood sweep efficiency through induced fines migration", J. Can. Pet. Technol., SPE-140141-PA, 2011, 50, 9–10 82–94.
[8] Gabriel G.A., Inamdar G.R., An experimental investigation of fines migration in porous media, Paper presented at the SPE Annual Technical Conference and Exhibition, San Francisco, California, October 1983. doi: https://doi.org/10.2118/12168-MS
[9] Okechukwu A.E., Sunday E.E., Abdulaziz A.M., Namdie J.I., Ubong R.W., Estimation of Original Oil in Place Using Pickett's and Buckle's Plots, Offshore Niger Delta, Nigeria. Petroleum and Coal, 2020, 62(4), 1279 – 1288. https://www.vurup.sk/wp-content/uploads/2020/10/PC-X_-Ebuka_109_rev2.pdf
[10] Khilar K.C., Fogler H.S., Migrations of Fines in Porous Media xiii" Kluwer Academic Publishers, Dordrecht; Boston, 1998, p. 171.
[11] Gruesbeck C., Collins R.E., Entrainment and deposition of fine particles in porous media, J. Petrol. Technol., 1982, 22 (6) 847–856. doi: https://doi.org/10.2118/8430-PA
[12] Abdulridha H.L.; Abdulaziz A.M.; Khalil A.A.; Alhussainy S.; Askar A.S.A.; Dahab A.S.A.; Alfarge D., Study on uncertainty analysis for drilling engineering applications: Wellbore stability assessments, Arabian Journal for Science and Engineering, 47 (9), 11687, 2022, 10.1007/s13369-021-06389-7
[13] Ahmadi M., Habibi A., Pourafshary P., Zeta potential investigation and mathematical modeling of nanoparticles deposited on the rock surface to reduce fine migration, Presented at SPE Middle East Oil and Gas Show and Conference, Manama, Bahrain, SPE-142633-MS, 2011. doi: https://doi.org/10.2118/142633-MS
[14] Binshan, Ju, Shugao, Dai, Zhian, Luan, Tiangao, Zhu, Xiantao, Su, and Qiu Xiaofeng, A Study of Wettability and Permeability Change Caused by Adsorption of Nanometer Structured Polysilicon on the Surface of Porous Media, Paper presented at the SPE Asia Pacific Oil and Gas Conference and Exhibition, Melbourne, Australia, October 2002. doi: https://doi.org/10.2118/77938-MS
[15] Kelsall R., Hamley I., Geoghegan M., Nanoscale science and technology, John Wiley & Sons Ltd, Chichester, West Sussex PO19 8SQ, England, 2005, pp. 456
[16] El-Diasty A.I., Salem A.M. (2013): Applications of Nanotechnology in the Oil and Gas industry: Latest Trends worldwide and Future Challenges in Egypt, " Paper presented at the North Africa Technical Conference and Exhibition, Cairo, Egypt, April 2013. doi: https://doi.org/10.2118/164716-MS

[17] Huang T., Crews B.J., Willingham J.R., Nanoparticles for formation fines fixation and improving performance of surfactant structure fluid, Paper presented at the International Petroleum Technology Conference, Kuala Lumpur. Malaysia, December 2008. doi: https://doi.org/10.2523/IPTC-12414-MS
[18] Ogolo N.A, Onyekonu M.O., Akaranta O., Trapping mechanism of nanofluids on migrating fines in sand, Paper presented at the SPE Nigeria Annual International Conference and Exhibition, Lagos, Nigeria, August 2013. doi: https://doi.org/10.2118/167502-MS
[19] Hasannejad R., Pourafshary P., Vatani A., Sameni A., Application of silica nanofluid to control initiation of fines migration, Petroleum Exploration and Development, 2017, 44 (5), 850–859. https://doi.org/10.1016/S1876-3804(17)30096-4
[20] Abhishek I.D.R., Hamouda A.A., Effect of various silica nanofluids: reduction of fines migrations and surface modification of Berea sandstone, Appl. Sci., 2017, 7(12), 1216; https://doi.org/10.3390/app7121216
[21] Habibi A., Ahmadi M., Pourafshary P., Fines migration control in sandstone formation by improving silica surface Zeta potential using a nanoparticle coating process", Energy Sources, 2014, 36 (21), 2376–2382. https://doi.org/10.1080/15567036.2011.569836
[22] El Neiri M.H.; Dahab A.S.A.; Abdulaziz A.M., The dynamic underbalanced drilling: A new drilling technique, Proceedings of the SPE/IADC Middle East Drilling Technology Conference and Exhibition, 2016, 10.2118/178153-ms
[23] Assef Y., Arab D., Pourafshary P., Application of nanofluid to control fines migration to improve the performance of low salinity water flooding and alkaline flooding, Journal of Petroleum Science and Engineering, 124, 2014, pp. 331-340, https://doi.org/10.1016/j.petrol.2014.09.023
[24] Youssif M.I., El-Maghraby R.M., Saleh S.M., El-gibaly A., Silica nanofluid flooding for enhanced oil recovery in sandstone rocks. Egyptian Journal of Petroleum, 27 (1), 2018, pp. 105-110, https://doi.org/10.1016/j.ejpe.2017.01.006
[25] Wasan D., Nikolov A., Kondiparty K., The wetting and spreading of nanofluids on solids, Role of the structural disjoining pressure, Current Opinion in Colloid & Interface Science,16 (4), 2011, P. 344-349. https://doi.org/10.1016/j.cocis.2011.02.001
[26] McElfresh P.M., Holcomb D.L., Ector D., Application of nanofluid technology to improve recovery in oil and gas wells, Paper presented at the SPE International Oilfield Nanotechnology Conference and Exhibition, Noordwijk, The Netherlands, 2012. doi: https://doi.org/10.2118/154827-MS
[27] Chengara A., Nikolov A.D., Wasan D.T., Trokhymchuk A., Henderson D., Spreading of nanofluids driven by the structural disjoining pressure gradient, Journal of Colloid and Interface Science, 280, (1), 2004, P. 192-201 https://doi.org/10.1016/j.jcis.2004.07.005
[28] Roustaei A., Moghadasi J., Iran A., Bagherzadeh H., Shahrabadi A., *An Experimental Investigation of Polysilicon NP Recovery Efficiencies through Changes in Interfacial Tension and Wettability Alteration*, Paper #SPE-156976-MS presented at the SPE International Oilfield Nanotechnology Conference and Exhibition, Noordwijk, The Netherlands, 2012. https://doi.org/10.2118/156976-MS
[29] Shidong L., Luky H. , Torsaeter O., *"Improved Oil Recovery by Hydrophilic Silica Nanoparticles Suspension: 2-Phase Flow Experimental Studies*." Paper presented at the International Petroleum Technology Conference, Beijing, China, 2013. doi: https://doi.org/10.2523/IPTC-16707-MS
[30] Shidong L., Ole T., (2014): *An Experimental Investigation of EOR Mechanisms for Nanoparticles Fluid in Glass Micromodel*, this paper was prepared for presentation at the International Symposium of the Society of Core, Analysts held in Avignon, France, 2014. DOI: 10.13140/RG.2.1.4181.3604
[31] Rafael R., Javier P., Alberto M., Arthur M., Diego S., and Abuseif H., *An Alternative Solution to Sandstone Acidizing Using a Nonacid-Based Fluid System with Fines-Migration Control*, Paper presented at the SPE Annual Technical Conference and Exhibition, Anaheim, California, U.S.A., 2007. doi: https://doi.org/10.2118/109911-MS
[32] Dahab A.S., Abdulaziz A.M., Manhalawi, A.A., Ahmed K., AL-Husseini, N., *Managing wellbore instability through geomechanical modeling and wellbore stability analysis.* Paper #164331presented in the 54th U.S. Rock Mechanics/Geomechanics Symposium, Virtual Online meeting, 2020, p. 2205-2214
. https://api.semanticscholar.org/CorpusID:225030512
[33] Wang Y., Yu M., Le-Hussain F., *Effect of Temperature on Fines Migration during Water Disposal,* Paper presented at the International Petroleum Technology Conference, Dhahran, Kingdom of Saudi Arabia, 2020.doi: https://doi.org/10.2523/IPTC-19826-MS
[34] Ibrahim M.M., Abdulaziz A.M., Fattah K.A., *STOIIP validation for a heterogeneous multi-layered reservoir of a mature field using an integrated 3D geo-cellular dynamic model,* Egyptian Journal of Petroleum, 27(4), 2018, pp. 887-896. https://doi.org/10.1016/j.ejpe.2018.01.004
[35] Salem K.G.S., Abdulaziz A.M., Dahab A.S., *Prediction of Hydraulic Properties in Carbonate Reservoirs Using Artificial Neural Network*, Paper presented at the Abu Dhabi International Petroleum Exhibition & Conference, Abu Dhabi, UAE, 2018.doi: https://doi.org/10.2118/193007-MS
[36] Brewer A., Dror I., Berkowitz B., *The mobility of plastic nanoparticles in aqueous and soil environments: a critical review.* ACS ES&T Water, 1 (1), 2021, pp. 48-57. doi: 10.1021/acsestwater.0c00130
[37] Hul G., Martignier A., Ramseier Gentile S., Zimmermann S, Ramaciotti P., Perdaems P., Stoll S., *Insights into polystyrene nanoplastics adsorption mechanisms onto quartz sand used in drinking water treatment plants*, Science of The Total Environment, 908, 2024, https://doi.org/10.1016/j.scitotenv.2023.16807
[38] Zhang Y., Diehl A., Lewandowski A., Gopalakrishnan K., Baker T., *Removal efficiency of micro- and nanoplastics (180 nm-125 μm) during drinking water treatment*. Sci. Total Environ., 720, 2020, https://doi.org/10.1016/j.scitotenv.2020.137383

[39] Arenas R.L., Gentile R.S., Zimmermann S., Stoll S., *Fate and removal efficiency of polystyrene nanoplastics in a pilot drinking water treatment plant,* Sci. Total Environ., 813, 2022, https://doi.org/10.1016/j.scitotenv.2021.152623
[40] Lyklema J., *Fundamentals of Interface and Colloid Science: Volume 1 (Fundamentals),* UK, Academic Press, 2000, pp.250
[41] Kosmulski M., *pH-dependent surface charging and points of zero charge. IV. Update and new approach,* Journal of Colloid and Interface Science, 337 (2), 2009, pp. 439-448, https://doi.org/10.1016/j.jcis.2009.04.072
[42] Kandil M.M., Abdulaziz A.M. El-Maghraby R.M., Youssef A.M., *Characterizations of a New Polymer-Nanocomposite Proppant from Agro-Waste Products for Hydraulic Fracturing Operations*. Egy. J. Chem., 68(2-2), 2025, pp. 561-572. doi: 10.1021/es802628n
[43] Bedrikovetsky P., Siqueira D.F., Furtado A.C. et al., *Modified Particle Detachment Model for Colloidal Transport in Porous Media,* Transp Porous Med 86, 2011, 353–383. https://doi.org/10.1007/s11242-010-9626-4
[44] Abdulaziz A., Microseismic monitoring of the hydraulic-fracture growth and geometry in the Upper Bahariya member, Khalda concession, Western Desert, Egypt, Journal of Geophysics and Engineering, 11(4), 45013, 2014. 10.1088/1742-2132/11/4/045013
[45] Jirjees, A.Y., Abdulaziz, A.M., *Influences of uncertainty in well log petrophysics and fluid properties on well test interpretation: An application in West Al Qurna Oil Field, South Iraq,* Egy. J. Petrol., 28(4), 2019, pp. 383–392. https://doi.org/10.1016/j.ejpe.2019.08.005
[46] Abdulaziz A.M.; Abdulridha H.L.; Dahab A.S.A.; Alhussainy S.; Abbas A.K., 3D mechanical earth model for optimized wellbore stablity, a case study from South of Iraq, Journal of Petroleum Exploration and Production Technology, 11 (9), 2021, 10.1007/s13202-021-01255-6
[47] Hul G., Gentile S.R., Zimmermann S., Stoll S., *Towards a better understanding of CeO2 manufactured nanoparticles adsorption onto sand grains used in drinking water treatment plants, Colloids and Surfaces,* A: Physicochemical and Engineering Aspects, 2022, https://doi.org/10.1016/j.colsurfa.2022.129000
[48] Fu J., Chen Z., Wang M., Liu S., Zhang J., Zhang J., Han R., Xu Q., *Adsorption of methylene blue by a high-efficiency adsorbent (polydopamine microspheres): Kinetics, isotherm, thermodynamics and mechanism analysis,* Chemical Engineering Journal, 259, 2015, pp. 53-61, https://doi.org/10.1016/j.cej.2014.07.101.
[49] Singh N., Tiwari E., Khandelwal N., Darbha G.K., *Understanding the stability of nanoplastics in aqueous environments: effect of ionic strength, temperature, dissolved organic matter, clay, and heavy metals.* Environ. Sci. Nano, 6 (10), 2019, pp. 2968-2976.
https://pubs.rsc.org/en/content/articlelanding/2019/en/c9en00557a
[50] You Z., Badalyan A.,Yang Y., Bedrikovetsky P., Hand M., *Fines Migration in Geothermal Reservoirs: Laboratory and Mathematical Modelling,* Geothermics; 77, 2019, pp. 344–36, https://doi.org/10.1016/j.geothermics.2018.10.006
[51] Huang L., Fang H., Chen M., *Experiment on surface charge distribution of fine sediment.* SCIENCE CHINA Technol. Sci., 55 (4), 2012, pp. 1146-1152. https://doi.org/10.1007/s11431-011-4730-4
[52] Loosli F., Le Coustumer P., Stoll S., *TiO2 nanoparticles aggregation and disaggregation in presence of alginate and Suwannee River humic acids. pH and concentration effects on nanoparticle stability.* Water Res., 47 (16), 2013, pp.6052-6063. https://doi.org/10.1016/j.watres.2013.07.021
[53] Ibrahim M.M., Abdulaziz A.M., Fattah K.A., 2016. *Rejuvenation of a Mature Field Through STOIIP Validation Using an Integrated 3D Geo-Cellular Dynamic Model for a Heterogeneous Multi Layered Reservoir,* Paper presented at the Abu Dhabi International Petroleum Exhibition & Conference, Abu Dhabi, UAE, 2016. https://doi.org/10.2118/183565-MS
[54] Abdulaziz A.M., Hawary S.S., *Prediction of carbonate diagenesis from well logs using artificial neural network: An innovative technique to understand complex carbonate systems*, A.Sh.Eng. J., 11(4), 2020, pp. 1387–1401. https://doi.org/10.1016/j.asej.2020.01.010
[55] Mansour M., Eleraki M., Noah A., Moustafa E., *Using nanotechnology to prevent fines migration while production*. Petroleum, 7 (2), 2021, pp. 168-177.